ELSEVIER

Journal of Molecular Catalysis A: Chemical 132 (1998) 101–112

JOURNAL OF MOLECULAR CATALYSIS A: CHEMICAL

# Kinetics of alkane adsorption on a solid cracking catalyst

Yury V. Kissin *

*Gulf Research and Development Co., Pittsburgh, PA, USA*

Received 22 May 1997; accepted 3 October 1997

**Abstract**

A microreactor technique is developed for a study of alkane chemisorption on solid cracking catalysts. Kinetics of adsorption–desorption processes can be observed at ca. 200°C; it manifests itself as extensive tailing of alkane peaks in gas chromatograms. A kinetic model of the adsorption process is developed. The model allows calculation of two kinetic parameters, those of alkane adsorption, $k_a[C^*]$, and desorption, $k_d$. Both these values decrease as the carbon atom number of an alkane increases. In a first approximation, both the $k_a$ and $k_d$ values for an alkane with a given carbon atom number do not depend on the degree of chain branching. All these features are typical for chemisorption, i.e. strong, non-specific interaction of alkane molecules with particular areas on the catalyst surface situated within its zeolite component. The experimental technique and the kinetic approach for measuring rapid adsorption–desorption phenomena described in this article can be applied to a variety of catalytic processes involving gas/solid interactions. 

*Keywords:* Catalytic cracking; Alkanes, adsorption; Alkanes, cracking; Adsorption, by cracking catalysts

## 1. Introduction

Chemisorption of alkanes on the surfaces of solid zeolite-based cracking catalysts is usually regarded as the first step in their cracking reactions [1–5]. A number of publications is devoted to zeolite adsorption studies of polar compounds, in particular, water [3–7], alcohols and phenols [8,9], as well as aromatic compounds [5,10–12] and oxygen [13]. Theoretical models of such adsorption phenomena have also been developed [3,14]. The early research on adsorption of saturated alkanes [9,15] was mostly concerned with equilibrium phenomena; however, several recent articles provided a detailed analysis of associated kinetic effects [16–19].

Earlier we described a simple microtechnique for the measurement of relative alkane reactivities and the primary product formation in alkane cracking reactions in the 250–400°C range [20–22]. This technique provides a convenient means for working with very small amounts of numerous hydrocarbons, both single feeds and mixtures. This article describes the use of this technique for the kinetic study of alkane adsorption phenomena over a solid cracking catalyst.

* Corresponding author. Present adress: Mobil Chemical Co., P.O. Box 3029, Edison, NJ 08818-3029, USA.

1381-1169/98/$19.00 
*PII* S1381-1169(97)00236-7

The experimental technique used in this study is, in effect, equivalent to a flow of a pulse of an evaporated sorbate over the packed column of a sorbent. Such arrangements, in general, represent a complex kinetic problem which is applicable to chromatographic separations, transport processes in solid-layer, fluidized-bed and tubular chemical reactors, etc. [23]. The principal difficulty in analyzing adsorption–desorption phenomena in the packed layer of a sorbent is the overlap of adsorption–desorption processes and transport phenomena of sorbates, such as internal mass-transfer resistance, intracrystalline diffusion in catalyst granules (they consist of a true adsorbent, a zeolite, and an inert binder), axial spreading of the feed pulse in the layer, etc. Therefore, any analysis of experimental data should take into account numerous macroscopic effects, including the pressure gradient across the packed layer, the presence of a dead volume in the column and in the apparatus itself, the flow rate of a carrier gas, etc. [16,18,23].

However, most of the macroscopic effects can be effectively minimized if a packed column is very short and if the sorbate concentration in the gas flow is very low. Chiang et al. [16,17] demonstrated that quantitative analysis of an eluted peak shape affords evaluation of controlling factors in the overall transport process. As shown below, our experimental arrangement corresponds to such a limiting case when all macroscopic gas transport processes are fast and the peak shape of eluted alkanes is predominantly controlled by adsorption–desorption phenomena themselves.

## 2. Experimental

A gas chromatograph, Hewlett-Packard 5880A, equipped with an FID detector was used both as a reactor and as an analytical tool. A small load of a catalyst (ca. 0.05 g) was placed on the frit of the glass tube in the injection assembly of the chromatograph. It produced a very short packed layer, 2–3 mm in length. The catalyst was overlaid with a 2–3 mm layer of an inert high-surface powder which is traditionally used in gas chromatography to facilitate sample evaporation (10% OV-1 on 80–100 mesh SW-AW-DMCS). The catalyst was dried in a He flow at 200°C for several hours. To study alkane adsorption in the catalyst layer, the injection assembly was heated to 190 or 200°C and 0.2 $\mu$l of a hydrocarbon mixture containing 8 alkanes dissolved in $n$-$C_6$ was injected into the space above the catalyst layer. The feed contained four linear alkanes, $n$-$C_8$, $n$-$C_{10}$, $n$-$C_{11}$ and $n$-$C_{12}$; three 2-methyl-branched alkanes, 2-Me-$C_8$, 2-Me-$C_9$ and 2-Me-$C_{10}$, and one dimethyl-branched alkane, 2,7-$Me_2$-$C_8$; each alkane at ca. 5 wt% concentration in the mixture.

The feed evaporated and produced a gas mixture containing ca. 0.1 mmol of hydrocarbon vapor per liter of gas. The pulse of the alkane vapor was carried by the He flow through the catalyst layer at a linear speed of 13 cm/s. At the employed feed/catalyst ratios, each $C_8$–$C_{12}$ alkane molecule had ca. 2000 $A^2$ of the zeolite surface available for adsorption. The plug of the alkane vapor contacted the catalyst for a period of ca. 1 s and then immediately entered a chromatographic column. The column was a 50 m, 0.2 mm i.d. capillary (PONA) coated with a 0.5 $\mu$m film of cross-linked methyl silicone. The He flow rate was 1 cc/min and the column temperature was kept constant at 50°C throughout each experiment which lasted for ca. 40 min.

Two catalysts were tested. The first was a commercial steam-equilibrated cracking catalyst FSS-1 (Filtrol). It contained ca. 20% of the rare earth-exchanged Y zeolite with $S_o$ of 400–500 $m^2/g$. The second catalyst was amorphous silica–alumina AAA calcined for 12 h at 540°C.

The fitting of kinetic models and experimental data was performed with a non-linear least-square computer program MINSQ2 from MicroMath Scientific Software.

## 3. Results

### 3.1. Manifestations of alkane adsorption

When the injection tube of the chromatograph contained only catalytically inert powder (the same amount as that of a catalyst), the chromatogram of the alkane mixture differed very little from the standard gas chromatogram (Fig. 1). Due to relatively low evaporation temperatures, 190–200°C, the peaks have the shape of a narrow rectangular triangle with a steeply inclined front edge and the end edge nearly perpendicular to the baseline, with no tailing (Fig. 1). The half-widths of all peaks were ca. 3 s. When the zeolite-based cracking catalyst was placed in the injection tube, the peak shapes of the eluding hydrocarbons were very different. Fig. 1 shows the *n*-$C_{12}$ range of the chromatogram of the alkane mixture which contacted the catalyst at 190°C. The chromatogram has two distinct features. The first one is the narrow peak of the alkane passing through the catalyst layer without impediment. The peak has the same elution time, 27.4 min. The second feature in the chromatogram is a broad, asymmetric peak with a relative elution time exceeding 5 min. We interpret this broad peak as a manifestation of alkane adsorption in the catalyst. Most of the alkane molecules (ca. 96%, judging by relative areas of the two peaks) are captured in the catalyst bed and in a process of slow desorption and re-adsorption, gradually migrate through the catalyst layer and emerge from it after a significant delay. GC peaks of other alkanes have similar shapes, their widths vary from 2 to 4 minutes. Fortunately, tails of all peaks do not overlap with the peaks of other alkanes.

The following general features of the alkane adsorption phenomena are important:

(1) Desorption peaks similar to that shown in Fig. 1 were observed for all alkanes in the mixture, both at 190 and 200°C. The peaks differ each from other in the rate of desorption, as described below. In most cases, the peaks of alkane molecules which pass through the catalyst layer without adsorption overlap with front edges of the adsorption–desorption peaks.

(2) Alkane desorption at increased temperatures (e.g. 250°C) occurs much faster and it manifests itself mostly in excessive tailing of GC peaks.

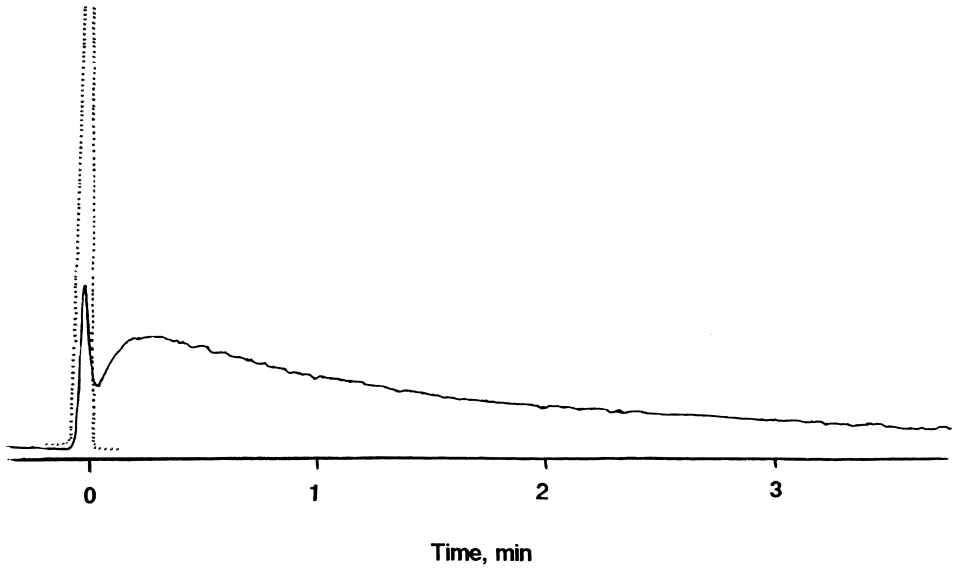


Fig. 1. Gas chromatograms of *n*-dodecane recorded with inert powder (dotted line) and the cracking catalyst (solid line) in the injection tube. The abscissa gives the relative retention time with respect to the elution time of the free alkane.

(3) The adsorption phenomena at 190–200°C are not accompanied by any chemical reactions. Alkane isomerization becomes noticeable only at 250°C [20,21] and significant alkane cracking to lighter products usually requires even higher temperatures.

(4) Alkanes are mostly adsorbed by the zeolite component in the catalyst. When amorphous silica–alumina was tested, the alkane adsorption was barely noticeable as slightly excessive tailing of GC peaks.

### *3.2. Kinetic scheme*

The first necessary stage in the quantitative analysis of broad elution peaks such as that shown in Fig. 1 is to differentiate between true adsorption–desorption phenomena of alkanes in the zeolite component of the catalyst and macroscopic processes related to transport of alkane vapor through the packed layer of a multi-component adsorbent. Two very sophisticated and complex solutions of this problem are described in the literature [16–19]. Computer simulation of elution peak profiles showed that different macroscopic phenomena affect the peak shape differently:

(1) Axial dispersion of a sorbate in the gas flow spreads the peak symmetrically [16]; the effect which is negligibly small for very short columns and which was never observed in our experiments in the catalyst absence.

(2) A pressure drop across the column can produce a noticeable peak tailing but, again, it is negligibly low for very short columns.

(3) A high gas flow rate is beneficial for producing narrow elution peaks and eliminating excessive peak tailing, as described by Chiang et al. [16]. This condition was adopted in the present study. The bed time constant $L/\mathrm{GV}$ where $L$ is the length of the catalyst layer and GV is the superficial gas velocity (see details below) in our experiments was of the order of 0.02 s, much smaller than the values which could cause significant tailing according to calculations in Ref. [16].

In general, the appearance of elution peaks in our experiments and, in particular, the existence of two peaks for some sorbates (as shown in Fig. 1), one narrow peak for molecules passing through the catalyst layer without adsorption and another delayed, broad and asymmetric peak of adsorbed molecules, corresponds to literature examples of transport processes controlled by adsorption–desorption processes [16,17].

A general kinetic description of an alkane desorption curve like that shown in Fig. 1 is quite complex. The following stages should be examined:

(1) A droplet of the alkane mixture, with a diameter of ca. 0.7 mm, is injected into a space above the catalyst layer held at 190–200°C and rapidly evaporates in the fast He flow. The evaporation kinetics is mostly determined by three factors; a rapidly increasing temperature of the droplet, its decreasing diameter due to evaporation and, most importantly, by the fact that *n*-hexane, the main component of the alkane mixture, evaporates nearly instantly under our conditions resulting in efficient dispersion of other hydrocarbons in the gas flow. An approximate computer modeling of the evaporation process showed that the evaporation lasts from 1 to 2 s at 200°C and that the concentration of the alkane vapor passes through a flat maximum close to the end of the evaporation period. Adequacy of this estimation is supported by the values of the GC peak half-widths in the catalyst absence, ca. 3 s, and the shapes of the peaks (Fig. 1).

(2) A stream of alkane vapor progresses in a plug-flow fashion through the catalyst layer which is 2–3 mm long. The contact time of the vapor pulse and the catalyst bed is very short. The linear rate of the gas flow through the tube with the catalyst in our experiments is 13 cm/s which means that the average time a given nonadsorbed alkane molecule spends in the catalyst layer is ca. 0.02 s. Nevertheless, due to a high adsorption rate, most of the alkane molecules are adsorbed on the catalyst surface.

(3) The total contact time between the plug

flow of the alkane vapor and the catalyst layer is of the order of 1 s. After that, adsorbed molecules start to desorb and, in a sequence of adsorption/desorption steps, slowly emerge at the end of the catalyst layer, pass the chromatographic column and their relative concentration in the gas stream is measured by a GC detector.

A thorough quantitative description of the overall transport phenomena in the pulse flow experiments through packed columns is very complex [16,18] and requires an extensive use of large computers. Presented below is an alternative kinetic analysis which is better suited for the study of catalytic reactions in very short packed columns under the assumption that the overall process is dominated by adsorption–desorption phenomena. Although this kinetic analysis also ultimately relies on the use of a personal computer, it affords, through a computer data-fitting process, a direct evaluation of kinetic parameters.

The analysis is based on the proposition that these two events, the initial adsorption of the alkane pulse by the catalyst layer and the subsequent desorption/re-adsorption process, are separated in time: the first stage lasts 1–2 s while the second stage occupies from 1 to 5 min.

*3.2.1. Initial alkane adsorption*

An alkane, in an amount of $S_0$ mol, forms a pulse of alkane vapor with an average concentration of $[S]_0^{\mathrm{v}}$ M:

$$[S]_0^{\mathrm{v}} = S_0/(\mathrm{CR}\cdot \mathrm{GV}\cdot t_{\mathrm{p}}) = S_0/V_{\mathrm{g}} \qquad (1)$$

where GV is the linear gas velocity ($\sim 13$ cm/s), CR is the cross-section area of the tube with the catalyst (0.126 $\mathrm{cm}^2$), $t_{\mathrm{p}}$ is the duration of the pulse, 1–2 s, and $V_{\mathrm{g}}$ is the volume of the alkane vapor plug ($\sim 0.002$ l). The amount of each alkane, $S_0$, injected in the gas stream over the catalyst layer is $\sim 5\cdot 10^{-8}$ mol and its average concentration, $[S]_0^{\mathrm{v}}$, is ca. $2\cdot 10^{-5}$ M.

The vapor plug moves through the catalyst layer of a length $L$ (0.2–0.3 cm) which contains $C^*$ mol of adsorption centers. The concentration of the adsorption centers in the catalyst bed is $[C^*] = C^*/(\mathrm{CR}\cdot L) = C^*/V_{\mathrm{c}}$, where $V_{\mathrm{c}}$ is the volume of the catalyst layer, $\sim 5\cdot 10^{-5}$ l. Alkane adsorption is assumed to be a simple bimolecular reaction which, due to a very small reaction time, is practically irreversible:

$$S + C^* \xrightarrow{k_{\mathrm{a}}} S_{\mathrm{a}} \qquad (2)$$

Here $S_{\mathrm{a}}$ represents an adsorbed alkane molecule and $k_{\mathrm{a}}$ is the bimolecular adsorption rate constant, l/mol · s. Because of very low substrate/catalyst ratios in our experiments, ca. 0.002–0.005, we assume that the alkane adsorption process occurs under the condition of $[S_0] \ll [C^*]$, i.e. one can neglect a decrease in the concentration of free adsorption centers $C^*$ as a result of adsorption of a small number of alkane molecules and assume that $[C^*] \sim$ constant.

Consider a particular cross-section of the catalyst layer at a distance $l$ cm from its front edge. It is convenient to use a nondimensional measure of the distance, $x = l/L$, with $x$ varying from 0 to 1. Under the steady-state assumption, each elemental catalyst layer $(x,\ x + \mathrm{d}x)$ at a distance $x$ from the front edge and with a thickness of $\mathrm{d}x$ (volume $\mathrm{d}V_{\mathrm{c}} = V_{\mathrm{c}}\mathrm{d}x$) is exposed to a stream of vapor with an approximately constant alkane concentration $[S]_x^{\mathrm{v}}$ for a period of $t_{\mathrm{p}}$ s. The $[S]_x^{\mathrm{v}}$ value varies from $[S]_0^{\mathrm{v}}$ (given by Eq. (1)) for the first elemental catalyst layer to a very low value for the last elemental layer. The elemental layer $(x,\ x + \mathrm{d}x)$ initially adsorbs a particular amount of the alkane, $(\mathrm{d}S_x^{\mathrm{a}})_0$, given by Eq. (3):

$$(\mathrm{d}S_x^{\mathrm{a}})_0 = k_{\mathrm{a}}\cdot [C^*]\cdot [S]_x^{\mathrm{v}}\cdot V_{\mathrm{c}}\cdot t_{\mathrm{p}}\cdot \mathrm{d}x \qquad (3)$$

As a result of adsorption, the alkane concentration in the plug flow gradually decreases. The decrease is described by Eq. (4) which equals the amount of the adsorbed alkane, $(\mathrm{d}S_x^{\mathrm{a}})_0$ in Eq. (3), and the loss of the alkane from the gas stream:

$$(\mathrm{d}S_x^{\mathrm{a}})_0 = -\mathrm{d}[S]_x^{\mathrm{v}}\cdot V_{\mathrm{g}} \qquad (4)$$

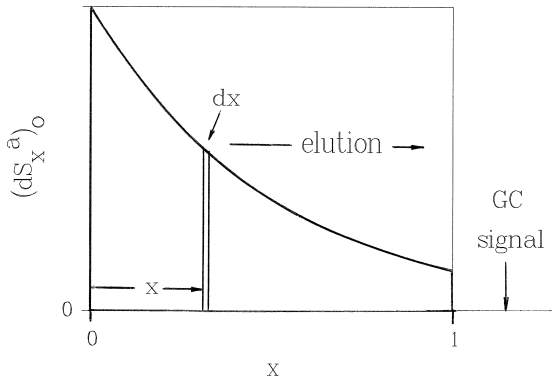


Fig. 2. Scheme of the distribution of an adsorbed alkane in the catalyst layer prior to the onset of alkane desorption (Eq. (6)).

Combining Eqs. (3) and (4) and integrating with respect to $[S]_x^v$ within limits $\{x\colon 0 \to 1;\ [S]_0^v \to [S]_x^v\}$ gives the following dependence for the alkane concentration in the gas phase as a function of $x$:

$$[S]_x^v = [S]_0^v \cdot \exp\left[-k_a \cdot [C^*] \cdot (V_c/V_g) \cdot t_p \cdot x\right] \quad (5)$$

Combining Eqs. (1), (3) and (5) gives the final expression for the initial distribution of the adsorbed alkane along the catalyst layer:

$$(dS_x^a)_0 = k_a \cdot [C^*] \cdot S_0 \cdot (V_c/V_g) \cdot t_p \cdot \exp\left[-k_a \cdot [C^*] \cdot (V_c/V_g) \cdot t_p \cdot x\right] dx \quad (6)$$

Eq. (6) signifies that the amount of alkane molecules initially adsorbed in an elemental layer $(x,\ x + dx)$ decreases exponentially with $x$, see Fig. 2.

In some instances, the fraction of the adsorbed alkane can be easily determined from experimental data (Fig. 1). This fraction, $F$, is defined as: $F$ = area of the desorption peak/total area of both peaks.

The kinetic model presented above gives the $F$ value as the ratio of the integral of Eq. (6) and $S_0$:

$$F = \left[\int_0^1 (dS_x^a)_0\right]/S_0 = 1 - \exp\left\{-k_a \cdot [C^*] \cdot (V_c/V_g) \cdot t_p\right\} \quad (7)$$

For such cases, Eq. (6) can be simplified by combining it with Eq. (7):

$$(dS_x^a)_0 = S_0 \cdot \ln[1/(1-F)] \cdot \exp\{-x \cdot \ln[1/(1-F)]\}\, dx \quad (8)$$

*3.2.2. Slow desorption stage*

After the end of the fast initial alkane adsorption stage (1–2 s), the second, much slower stage begins. The alkane molecules deposited in each elemental layer $(x,\ x + dx)$ desorb and slowly migrate through the remaining layer of the catalyst, $1 - x$. The rate of desorption follows the first-order kinetic law:

$$S_a \xrightarrow{k_d} S + C^* \quad (9)$$

where $k_d$ is the monomolecular desorption rate constant, $s^{-1}$. At any moment $t$, the amount of the remaining adsorbed molecules is given by:

$$(dS_x^a)_t = (dS_x^a)_0 \cdot \exp(-k_d \cdot t) \quad (10)$$

where $(dS_x^a)_0$ is defined by Eq. (6) or Eq. (8). Therefore, the desorption rate from the $(x,\ x + dx)$ layer is:

$$(dS_x)_t/dt = k_d \cdot (dS_x^a)_t = k_d \cdot (dS_x^a)_0 \cdot \exp(-k_d \cdot t) \quad (11)$$

Subsequent to their release, the alkane molecules progress through the remaining part of the catalyst layer in a series of adsorption–desorption steps. A detailed kinetic description of this process is complex. It can be most easily handled if the movement of alkane molecules through the catalyst layer is described in terms of their residence time in the layer.

When several alkane molecules are simultaneously released from a $(x,\ x + dx)$ elemental layer, they, due to statistical nature of their migration through the catalyst bed, will arrive at the end of the layer $(x = 1)$ at different times $\vartheta$. The average speed of this migration can be defined in terms of average residence times, $\tau_x$, of alkane molecules in the catalyst layer. We

postulate that the $\tau_x$ value for an alkane molecule desorbed at a distance $x$ from the front edge of the catalyst layer (the average time of the molecule's travel through the remaining length of the catalyst layer, $1-x$) is:

$$\tau_x = N \cdot \left(k_a \cdot [C^*]/k_d\right) \cdot (1-x) \qquad (12)$$

Eq. (12) signifies that the $\tau_x$ value is the function of the length of the remaining part of the layer, $1-x$, and of both the adsorption and desorption rate constants, with $N$ (s) being the normalization parameter. For a given molecule desorbed from the elemental catalyst layer ($x$, $x+\mathrm{d}x$), the relationship between the actual time of arrival at the end of the catalyst layer, $\vartheta$, and $\tau_x$ is defined by the probability function $(p_x)_\vartheta$. In accordance with the principles of chemical kinetics, the normalized $(p_x)_\vartheta$ function is exponential, with the $\tau_x$ value as the parameter:

$$(p_x)_\vartheta = \exp(-\vartheta/\tau_x)/\tau_x$$

$$\text{with } \int_0^\infty (p_x)_\vartheta \,\mathrm{d}\vartheta = 1 \qquad (13)$$

The GC detector signal (the ordinate in Fig. 1) is proportional to the combined rate of the arrival of all desorbed alkane molecules at the point of $x=1$. If only the molecules desorbed from the ($x$, $x+\mathrm{d}x$) elemental layer are measured (see the scheme in Fig. 2), the fraction of the total GC signal attributed to this layer, $\mathrm{d(GC)}_x$, at a time $T$ from the beginning of the desorption/re-adsorption stage is represented by the integral:

$$\left[\mathrm{d(GC)}_x\right]_T = \int_0^T (\mathrm{d}S_x)_t \cdot (p_x)_{T-t}\,\mathrm{d}t \qquad (14)$$

i.e. it is the integral function of the rate of alkane desorption at a particular time $t$ from the start of the experiment multiplied by the probability for the desorbed molecules to reach the end of the catalyst layer for the remaining time $\vartheta = T-t$. The desorption rate from the ($x$, $x+d\mathrm{x}$) layer (the $(\mathrm{d}S_x)_t$ value in Eq. (14)) is given by Eq. (11) and the probability $(p_x)_{\vartheta=T-t}$ is given by Eq. (13). Integration of Eq. (14) (it requires the use of Eqs. (10) and (13) and Eq. (6) or Eq. (8)) gives the following result:

$$\begin{aligned}\left[\mathrm{d(GC)}_x\right]_T = {} & k_d \cdot S_0 \cdot B \cdot \exp(-B\cdot x) \\ & \cdot \left[\exp(-T/\tau_x)/\tau_x\right] \\ & \cdot \left\{\left[1-\exp\left[-T\cdot(k_d - 1/\tau_x)\right]\right.\right. \\ & \left.\left./(k_d - 1/\tau_x)\right\}\mathrm{d}x\end{aligned} \qquad (15)$$

where $\tau_x$ is defined by Eq. (12) and $B$ is $k_a \cdot [C^*] \cdot (V_c/V_g)t_p$.

Again, as in the case of Eq. (6), Eq. (15) can be simplified if the initial alkane adsorption can be defined in terms of the fraction of initially adsorbed molecules $F$ (see derivation of Eqs. (7) and (8). In such a case, Eq. (15) is reduced to:

$$\begin{aligned}\left[\mathrm{d(GC)}_x\right]_T = {} & k_d \cdot S_0 \cdot \ln\left[1/(1-F)\right] \\ & \cdot \exp\left\{-x\cdot\ln\left[1/(1-F)\right]\right\} \\ & \cdot \left[\exp(-T/\tau_x)/\tau_x\right] \\ & \cdot \left\{1-\exp\left[-T\cdot(k_d - 1/\tau_x)\right\}\right. \\ & \left./(k_d - 1/\tau_x)\,\mathrm{d}x\right.\end{aligned} \qquad (16)$$

Finally, the expression for the total GC signal as a function of $T$ requires integration of $\left[\mathrm{d(GC)}_x\right]_T$ over the nondimensional thickness of the catalyst layer, $x$:

$$\mathrm{GC}_T = \int_0^1 \left[\mathrm{d(GC)}_x\right]_T \mathrm{d}x \qquad (17)$$

Integration of the right hand side in Eq. (15) or Eq. (16) with respect to $x$ cannot be achieved in the explicit form, but it is easily handled by computer.

### *3.3. Verification of kinetic scheme and estimation of rate constants*

Eqs. (15)–(17) contain the following independent parameters that can be determined by fitting Eq. (17) with the experimental data on alkane adsorption:

(1) For Eqs. (15) and (17): $k_a[C^*]$, $k_d$, $N$ (the parameter in $\tau$, Eq. (12)), $(V_c/V_g)t_p$ (in the range of 0.02–0.05 s) and a normalization parameter which is a combination of the $S_0$ value and the scale of the GC peak height. As typical in most cases of heterogeneous catalysis, $k_a$ and $[C^*]$ parameters cannot be separated in kinetic analysis and are measured as a product.

(2) For Eqs. (16) and (17): $k_a[C^*]$, $k_d$, $N$ and the normalization parameter. The $F$ value in such cases is measured independently from the GC data, as described above.

The experimental data shown in Fig. 1 provide a good test of the kinetic scheme. The $F$ value (the conversion in the initial adsorption reaction) for *n*-dodecane, calculated from the GC data, is 0.96. Eq. (17) with the $[d(GC)_x]_T$ function given by Eq. (16) was used to fit the experimental curve of Fig. 1. The results are shown in Fig. 3. The estimated parameters were: $k_a[C^*] = 0.23\ s^{-1}$, $k_d = 0.012\ s^{-1}$, $N = 0.40$ s. When, instead, the combination of Eqs. (15) and (17) was used for fitting, the calculations showed that the results were relatively insensitive to the $(V_c/V_g)t_p$ value in the range of 0.02–0.05 s and that the values of other fitted parameters were in the same ranges: $k_a[C^*] \sim 0.37\ s^{-1}$, $k_d \sim 0.013\ s^{-1}$, $N = 0.43$ s. Fig. 4 shows two more examples of the treatment of experimental kinetic data, those for *n*-undecane and 2-methyldecane at 190°C. A qualitatively similar but a much faster desorption process of *n*-decane from the bed of $La^{3+}$-Y zeolite at 300°C was described earlier [24] (measurement by the microgravimetric method with an inertial microbalance).

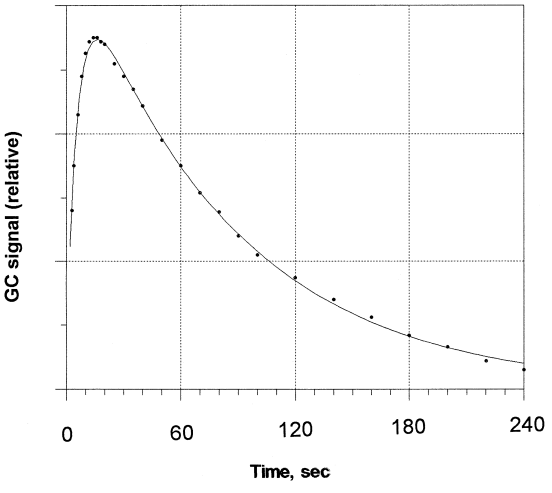


Fig. 3. Match between experimental data on *n*-dodecane desorption from the catalyst layer at 190°C (points, from Fig. 1) and the kinetic model (Eq. (17)).

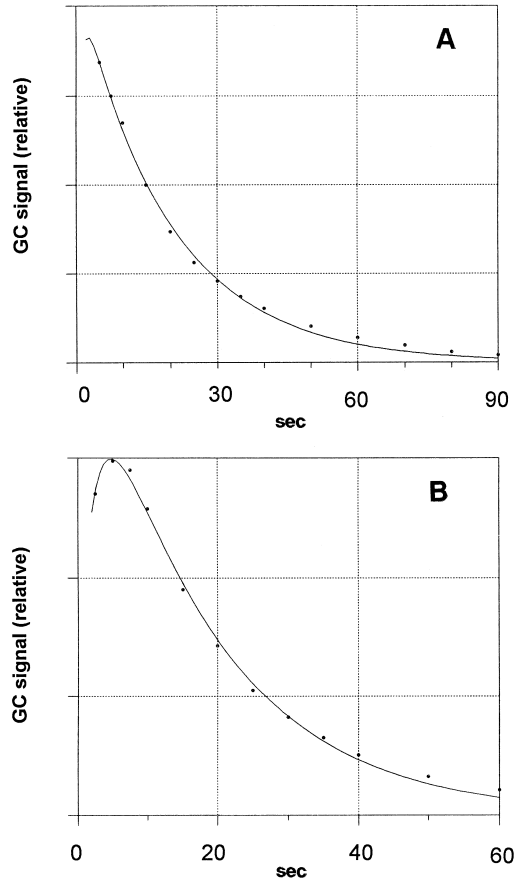


Fig. 4. Desorption kinetics of *n*-undecane (A) and 2-methyldecane (B) at 190°C.

In some cases, especially at higher temperatures and for lighter alkanes, the $k_a[C^*]$ value is quite high and cannot be reliably estimated anymore. Fig. 5 gives one example of the effect of the absolute values of adsorption and desorption rate constants on the reaction kinetics. Even if the equilibrium chemisorption constant $K$ remains the same (as in Fig. 5), when both the $k_a[C^*]$ and $k_d$ values increase, the maximums

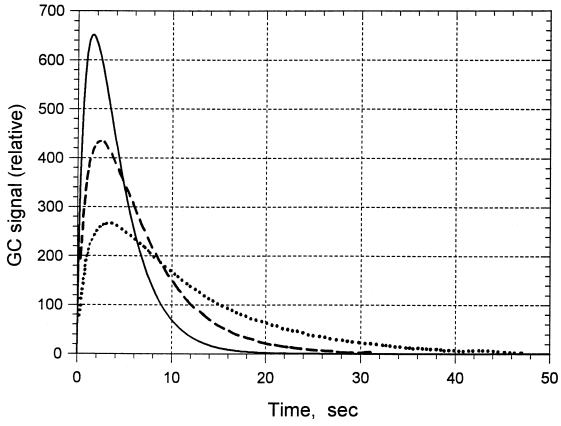


Fig. 5. Effect of absolute $k_a[C^*]$ and $k_d$ values on the kinetics of adsorption–desorption processes. Calculations were carried out with Eq. (7) for the same equilibrium constant $K$. Solid line: $k_a[C^*] = 4.0\ s^{-1}$, $k_d = 0.4\ s^{-1}$; dashed line: $k_a[C^*] = 2.0\ s^{-1}$, $k_d = 0.2\ s^{-1}$; points: $k_a[C^*] = 1.0\ s^{-1}$, $k_d = 0.1\ s^{-1}$.

Table 1
Kinetic parameters of alkane adsorption on zeolite-based cracking catalyst

| Temp. (°C) | Alkane | $k_a[C^*]$, $s^{-1}$ | $k_d$, $s^{-1}$ |
|---|---|---|---|
| 190 | *n*-octane | | 0.19 |
| | 2-methyloctane | | 0.17 |
| | *n*-decane | | 0.12 |
| | 2-methylnonane | | 0.11 |
| | 2,7-dimethyloctane | | 0.10 |
| | *n*-undecane | 0.60–0.66 | 0.052–0.055 |
| | 2-methyldecane | 0.65–0.71 | 0.057–0.058 |
| | *n*-dodecane | 0.23–0.37 | 0.012–0.013 |
| 200 | *n*-octane | | 0.27 |
| | 2-methyloctane | | 0.18 |
| | *n*-decane | | 0.14 |
| | 2-methylnonane | | 0.13 |
| | 2,7-dimethyloctane | | 0.11 |
| | *n*-undecane | 0.70 | 0.067 |
| | 2-methyldecane | 0.39 | 0.078 |
| | *n*-dodecane | 0.30 | 0.035 |

of the GC elution peaks shift closer to the peak positions of nonadsorbed alkanes (the half-widths of the latter are ca. 3 s) and overlap with them. In such cases, only the tails of the desorption curves can be analyzed and the kinetic scheme presented above is effectively replaced with a simple first-order desorption process:

$$GC_T = Q \cdot \exp(-k_d \cdot t) \quad (18)$$

where $Q$ is the normalization parameter of the peak area. In borderline cases, when both kinetic approaches can be utilized (a combination of Eqs. (15) and (17) versus Eq. (18)) the estimates of the $k_d$ values match within 10–15%.

## 4. Discussion

Table 1 lists kinetic parameters of alkane adsorption over the zeolite-based cracking catalyst. The following conclusions can be made from these data:

(1) Both the $k_a$ and the $k_d$ values strongly depend on the carbon atom number of an alkane. Because all alkanes were contacted with the catalyst layer together, one can assume that the $[C^*]$ term in the $k_a[C^*]$ product is constant in every experiment. Both the $k_a$ and $k_d$ values decrease as the carbon atom number increases.

(2) In the first approximation, the $k_d$ values for alkanes with a given carbon atom number do not depend on the degree of chain branching; compare, for example, $k_d$ values for different $C_{10}$ alkanes. The same can be also tentatively said about the $k_a[C^*]$ values (see the data for two $C_{11}$ alkanes); however, the precision of the $k_a$ estimation is not sufficient to make a definite conclusion.

(3) As expected, the $k_d$ value for a given alkane increases with temperature (the precision of the $k_a[C^*]$ value measurement is insufficient to draw any conclusions).

All these features indicate that the observed adsorption phenomena are best described as chemisorption, i.e. strong, non-specific interaction of alkane molecules with particular areas on the catalyst surface situated within its zeolite component. Alkane chemisorption is strong enough to manifest itself even at such high temperatures as 200°C. The phenomenon is not affected by the alkane structure and the strength of chemisorption is mostly determined by the

number of contact points between the zeolite surface and alkane molecules.

The lack of chain-structure sensitivity distinguishes alkane chemisorption from the next stage of catalytic cracking, formation of active species in cracking reactions. As we discussed earlier [20], relative reactivities of alkanes in catalytic cracking under mild conditions are proportional to the product of two kinetic parameters, the equilibrium chemisorption constant $K$ ($K = k_a/k_d$) and the rate constant of the active species formation, $k_1$. Table 2 compares these two kinetic parameters for three alkanes, *n*-undecane, 2-methyldecane and *n*-dodecane. The first parameter is the $k_a[C^*]/k_d$ ratio at 190°C calculated from the data in Table 1 and normalized to this ratio for *n*-undecane. The ratio represents the relative equilibrium adsorption constant $K$ for the alkanes. The second column in Table 2 lists relative reactivities of the same alkanes in cracking reactions over the same catalyst at 350°C [20]. In spite of the difference in reaction temperatures, this comparison supports the conclusions initially put forward in Ref. [20]:

(1) When linear alkanes are compared, their relative reactivities mostly depend on adsorption properties which are higher for high molecular weight alkanes.

(2) On the other hand, the much higher reactivities of branched alkanes compared to those of linear alkanes are mostly determined by the ease of the active species formation which is the function of the number of tertiary C–H bonds in isoalkanes [20–22,25].

The method described in the experimental part also provides an opportunity to observe chemisorption of olefins by cracking catalysts. Olefins are much more reactive in cracking reactions compared to alkanes and separate evaluation of their adsorption and chemical reactions is very difficult. Fig. 6 shows the gas chromatogram of 1-hexene passing over the layer of a fresh cracking catalyst at 100°C. Even at this low temperature, the double bond in the olefin is nearly completely isomerized with the preservation of the molecule's linear skeleton. The peaks of all isomers are asymmetrically

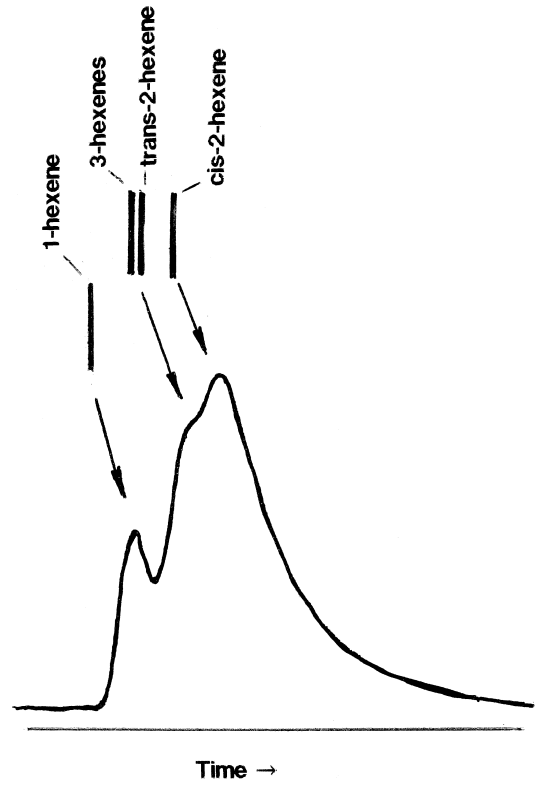


Fig. 6. Isomerization reactions of 1-hexene over the cracking catalyst and product desorption at 100°C. Bars show peak positions of respective alkenes in the absence of adsorption.

Table 2
Comparison of alkane adsorption and cracking over zeolite-based cracking catalyst

| Alkane | Relative adsorption equilibrium at 190°C (from $k_a[C^*]/k_d$) | Relative cracking reactivity at 350°C [20] $k_1K[C^*]t$ |
|---|---|---|
| *n*-Undecane | 1 | 1* |
| 2-Methyldecane | ~ 1.0 | 15.1 |
| *n*-Dodecane | ~ 2.0 | 2.0 |

* Extrapolated from data for *n*-alkanes $C_8$, $C_{10}$ and $C_{12}$.

broadened due to their low desorption rate constants. It should be noted that the kinetic treatment described in this article cannot be rigorously applied to such data because the chromatogram in Fig. 6 was recorded in the temperature-rising mode of the GC column at 5°C/min. This mode of operation, which is routinely used to make GC peaks more narrow, results in a faster elution of peak tails from a column compared to the constant-temperature mode adopted in this study, e.g. in Fig. 1.

In conclusion, one should note that the experimental technique and the kinetic approach for measuring rapid adsorption–desorption phenomena described in this article can be easily applied to a variety of catalytic processes involving gas/solid interactions. The main benefits of the technique are experimental simplicity, ability to compare adsorption of several compounds in a single experiment (provided that their GC peaks are sufficiently distant) and simplicity of kinetic calculations. The main disadvantage of the described method is the requirement of a quite short catalyst layer, a condition which complicates the measurement of absolute kinetic parameters.

## 5. Nomenclature

| | |
|---|---|
| $C^*$ | amount of adsorption centers in a catalyst layer (mol) |
| $[C^*]$ | concentration of adsorption centers in a catalyst bed (M) |
| CR | cross-section area of a catalyst layer ($cm^2$) |
| $F$ | fraction of adsorbed alkane |
| GC | normalized GC signal value |
| GV | linear gas velocity (cm/s) |
| $k_a$ | bimolecular adsorption rate constant ($l/mol \cdot s$) |
| $k_d$ | monomolecular desorption rate constant ($s^{-1}$) |
| $L$ | length of a catalyst layer (cm) |
| $N$ | normalization parameter in Eq. (12) (s) |
| $(p_x)_\vartheta$ | probability function of the residence time distribution |
| $S_a$ | amount of adsorbed alkane (mol) |
| $S_0$ | amount of alkane in pulse (mol) |
| $[S]_0^v$ | average concentration of alkane in gas stream (M) |
| $(dS_x^a)_0$ | initial amount of alkane adsorbed in the elemental layer $x$, $x + dx$ |
| $t_p$ | duration of a pulse (s) |
| $T$ | time from the appearance of the GC signal of the nonadsorbed alkane (s) |
| $V_c$ | volume of a catalyst layer (l) |
| $V_g$ | volume of an alkane vapor plug (l) |
| $x$, $x + dx$ | elemental section of a catalyst layer at a nondimensional distance $x$ from the top |
| $\vartheta$ | time of escape of a desorbed alkane molecule from a catalyst layer (s) |
| $\tau_x$ | average residence time of alkane molecules in a catalyst layer (s) |

## References


[1] B.C. Gates, J.R. Katzer, G.C.A. Schuit, Chemistry of Catalytic Processes, McGraw-Hill, New York, 1979.
[2] B.W. Wojciechowski, A. Corma, Catalytic Cracking: Catalysts, Chemistry and Kinetics, Marcel Dekker, New York, 1986.
[3] W.O. Haag, N.Y. Chen, in: L.L. Hegedus (Ed.), Catalyst Design-Progress and Perspectives, John Wiley and Sons, New York, 1987, ch. 6.
[4] N. Cardona-Martinez, J.A. Dumesic, in: D.D. Eley, H. Pines, P.B. Weisz (Eds.), Adv. Catal. 38 (1992) 169.
[5] P.B. Venuto, in: J. Weitcamp (Ed.), Microporous Materials, Elsevier, Amsterdam, 1993.
[6] R.M. Barrer, C.G. Bratt, Phys. Chem. Solids 12 (1959) 146.
[7] D.H. Olson, W.O. Haag, R.M. Lago, J. Catal. 61 (1980) 390.
[8] E. Narita, N. Horiguchi, T. Okabe, Chem. Lett. (1985) 787.
[9] R.M. Dessau, in: W.H. Flank (Ed.), Adsorption and Ion Exchange with Synthetic Zeolites, ACS Symposium Series No. 135, American Chemical Society, Washington, DC, 1987, ch. 8.
[10] P.B. Venuto, P.S. Landis, Adv. Catal. 18 (1968) 259.
[11] P.B. Venuto, E.L. Wu, J. Catal. 15 (1969) 205.
[12] E.L. Hopkins, J. Catal. 29 (1973) 112.
[13] W.S. Millman, C.H. Bartholomew, C. Richardson, J. Catal. 90 (1984) 10.
[14] R.M. Barrer, J. Colloid. Sci. 21 (1966) 415.

[15] M.L. Ocelli, F.S. Hwu, J.W. Hightower, Am. Chem. Soc. Meeting, Div. Petr. Chem. Abstr. New York, 1981, p. 672.
[16] A.S. Chiang, A.G. Dixon, Y.H. Ma, Chem. Eng. Sci. 19 (1984) 1451.
[17] A.S. Chiang, A.G. Dixon, Y.H. Ma, Chem. Eng. Sci. 19 (1984) 1461.
[18] L. Forni, C.F. Viscardi, C. Oliva, J. Catal. 97 (1986) 469.
[19] L. Forni, C.F. Viscardi, J. Catal. 97 (1986) 480.
[20] Y.V. Kissin, J. Catal. 126 (1990) 600.
[21] Y.V. Kissin, J. Catal. 132 (1991) 409.
[22] Y.V. Kissin, Catal. Lett. 19 (1993) 181.
[23] G.F. Froment, K.B. Bischoff, Chemical Reactor Analysis and Design, John Wiley, 1979, p. 163.
[24] F. Hershkovitz, H.S. Kheshgi, P.D. Madiara, Preprints, Am. Chem. Soc. Meeting, Symp. Adv. Fluid Catal. Cracking, vol. 38, No. 3, Chicago, 1993, p. 619.
[25] Y.V. Kissin, J. Catal. 163 (1996) 50.